

# Engineering Notes

ENGINEERING NOTES are short manuscripts describing new developments or important results of a preliminary nature. These Notes cannot exceed 6 manuscript pages and 3 figures; a page of text may be substituted for a figure and vice versa. After informal review by the editors, they may be published within a few months of the date of receipt. Style requirements are the same as for regular contributions (see inside back cover).

## Modeling of Nonlinear Human Operator in the Control Loop: Preliminary Results

Mario Innocenti,\* Andrea Balluchi,<sup>†</sup> and Aldo Balestrino<sup>‡</sup>  
University of Pisa, 56126 Pisa, Italy

### I. Introduction

MODELING of the human operator in the control loop has been an area of active research for quite some time.<sup>1</sup> In aerospace, automotive, and marine applications a human operator model (HOM) can be used to analyze system and subsystem performance and to help in the synthesis of components such as automatic controllers, displays, and manipulators. In addition, accurate models help in limiting the use of human operators during simulation, thus contributing to development cost reduction.

During tracking tasks when the operator is actively involved in the control of the plant, algorithmic models are available in the frequency domain<sup>1–3</sup> as well as in the time domain<sup>4–6</sup>; the interested reader can also refer to Ref. 7 for more information on the subject. The preceding models' primary characteristics are to extract the linear input-output behavior around crossover, which is then augmented by some physiological properties, most noticeably neuromuscular time delay and prediction capabilities. The models are essentially linear, and they have proved their capability in the operating frequency range of the system by numerous comparisons with experimental data.

The objective of the present work is to propose a HOM, when plant dynamics and/or input require a clear nonlinear strategy for performance as well as stability. Occurrences such as the preceding can be found when the system bandwidth is high and stability is critical, when the operator's actuation is close to saturation, and in aircraft applications when aircraft-pilot couplings known as pilot-induced oscillations are likely to occur. The motivation behind this is the absence of modeling of nonlinear behavior, as well as the fact that transition between linear and nonlinear control by the operator is an area where manual control is known to suffer loss of performance, increased workload, or both.

Current models were derived from a describing function approach,<sup>1</sup> where the nonlinear component (remnant) is negligible with respect to the linear one, or from linear-quadratic-regulator-based structures, with nonlinearity introduced as variable noise level.<sup>4</sup> All of these models however do not incorporate directly a discontinuous operator control activity, such as bang-bang, which occurs in many situations for instance during repeated transition from large amplitude control to fine tracking in piloted aircraft. To improve on current modeling, a novel model structure that uses sliding surfaces with delay is proposed here. The model is validated by limited experimental data and to identify the performance of different individuals, showing interesting properties for further development.

Received 27 January 1998; revision received 12 April 1999; accepted for publication 19 January 2000. Copyright © 2000 by the American Institute of Aeronautics and Astronautics, Inc. All rights reserved.

\*Professor, Department of Electrical Systems and Automation. Associate Fellow AIAA.

<sup>†</sup>Ph.D. Candidate, Department of Electrical Systems and Automation.

<sup>‡</sup>Professor, Department of Electrical Systems and Automation.

### II. Nonlinear Tracking Loop

A man-in-the-loop simulation facility was developed as part of a larger human performance modeling activity; more details on the actual setup are described elsewhere.<sup>8</sup> Although simple as setup, such facility is essential in generating experimental data necessary for modeling definition and validation. A schematic of compensatory display appearance is shown in Fig. 1, with the standard indicator on the right and additional indicators that provide information to the operator. The three boxes on the left are green, yellow, and red boxes indicating saturation of the command; the arrow points in the direction of reducing error. The capabilities of the simulation facility were tested over a variety of tracking experiments, with operators classified as trained, as well as untrained, and with linear plants taken from the literature. Matching of experimental data frequency response obtained with fast Fourier transform and Auto-Regressive Exogenous Input techniques was performed against the crossover model<sup>1</sup> and the optimal control model of the human behavior,<sup>3</sup> showing very good results.

The control loop considered in the paper is representative of a standard single-input single-output tracking task shown in Fig. 2. In

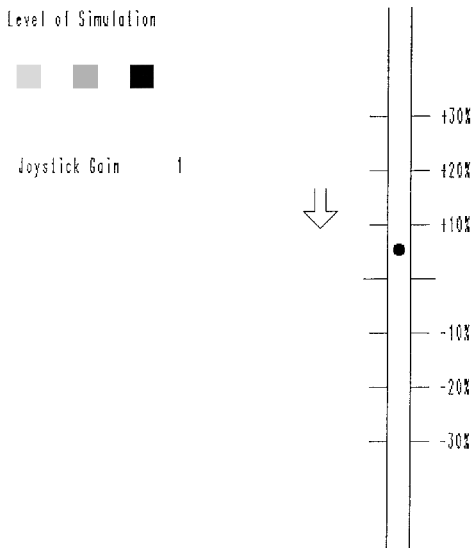


Fig. 1 Compensatory display.

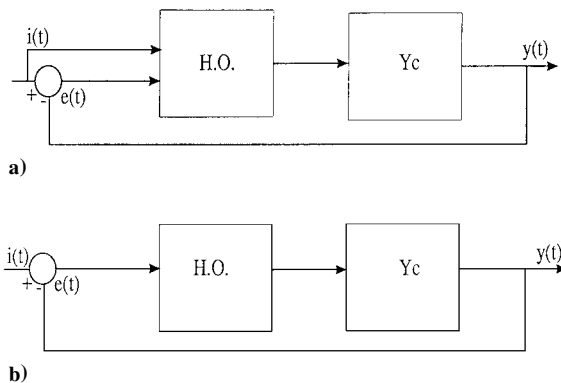


Fig. 2 Typical display in manual control tasks.

this preliminary work a compensatory display is used (see Fig. 2b), where the operator controls the plant based on a single display of the error between the reference signal to be tracked and the plant output. The plant used is a second-order system with transfer function  $Y_c(s)$ , having damping coefficient and resonant frequency values that are changed during the simulation campaign so as to excite a nonlinear behavior of the human operator, when appropriate selected pairs are chosen.

$$Y_c(s) = k / (s^2 + 2\xi\omega_0 s + \omega_0^2) \quad (1)$$

The input reference signal is a sine wave of the form  $i(t) = 2 \sin t$ . Although pure sinusoidal in nature, the input was tested experimentally in order to make sure that the operators would not perform their task in a precognitive fashion.

A set of experiments was carried out with different operators, who were asked to minimize the tracking error to the best of their ability, using their chosen control technique. An example of separation between linear and nonlinear behavior as function of plant dynamics is shown in Figs. 3 and 4 for two operators indicated by A and B, respectively. Operator A had been previously trained by performing the task several times, whereas B was an untrained operator.

The measure of linear and nonlinear behavior just used was chosen to be the ratio  $\gamma$  between the energy associated with the fundamental control frequency and remnant frequency as

$$\gamma = \frac{E_{\text{Fundamental}}}{(E_{\text{Total}} - E_{\text{Fundamental}})} \quad (2)$$

this value being consistent with linear and switching-type behavior observed in the experiments, with a selected threshold of  $\gamma =$

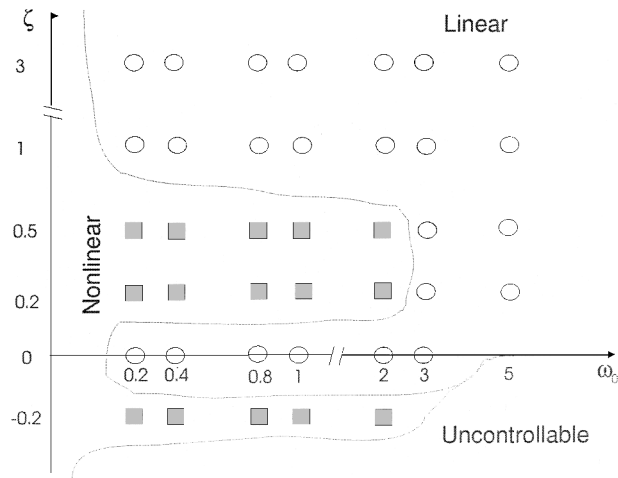


Fig. 3 Behavior of operator A in the controlled task.

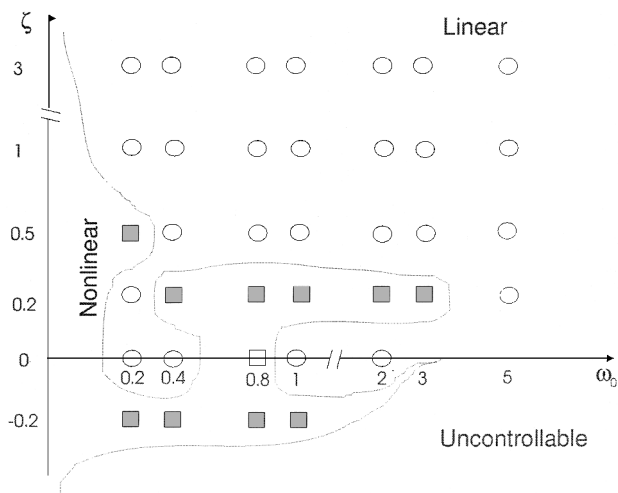


Fig. 4 Behavior of operator B in the controlled task.

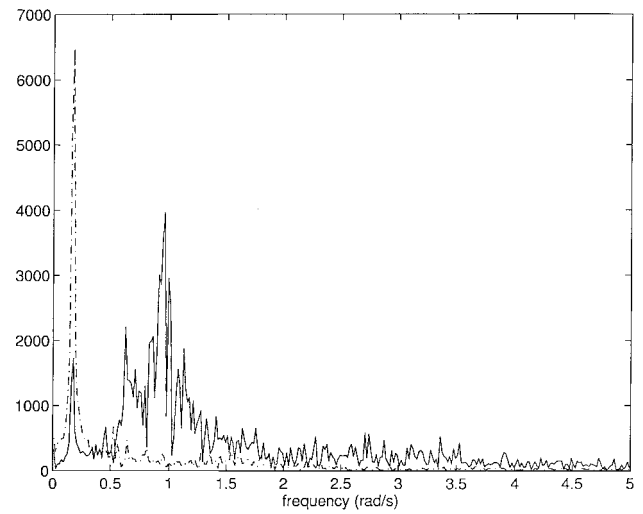


Fig. 5 Operator PSD: linear (---), nonlinear (cont.).

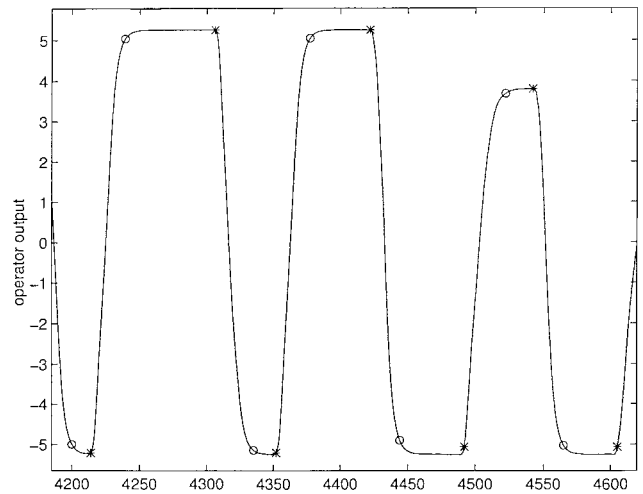


Fig. 6 Operator's control input.

−10 dB chosen based on the operators' comments. The difference between modes of control by the operator could also be found by comparing the control power spectral densities as shown in Fig. 5, where the dashed line indicates a linear manual control and the continuous line clearly shows a nonlinear behavior.

### III. Methodology and Model

Modeling considerations follow from the operators' behavior in the experiments described in the preceding section. If we consider a compensatory tracking task of system (1) with parameter values  $\omega_0 = 0.2$  rad/s and  $\xi = 0.5$ , a sample time history of the resulting control is shown in Fig. 6, where (o) indicates the saturation point and (\*) command switching of the manual control action. From the simulation some comments can be made:

- 1) The control is nonlinear of discontinuous type.
- 2) The control amplitude is not constant.
- 3) A delay is present in the control action.
- 4) The presence of a limit cycle that can be demonstrated from the simulation data<sup>8</sup> is a limit cycle.
- 5) During the saturated input cycle, the operators' bandwidth is very high and clearly beyond the typical linear range known to be up to 10–15 rad/s.

Based on the first comment, a sliding mode structure was considered as candidate model for the operator's behavior. The theoretical background in sliding modes is available in the literature.<sup>9,10</sup> Here we outline some of the major points for clarity's sake.

Consider a single input  $n$ -dimensional system of the form

$$\dot{x}^{(n)} = f(x) + b(x)u \quad (3)$$

where  $\mathbf{x}$  is the state vector and  $f(\mathbf{x})$  and  $b(\mathbf{x})$  are, in general, nonlinear functions with uncertainties bounded from above by known continuous functions of the state vector. A tracking problem requires the determination of a finite control  $u$  so that  $\mathbf{x}(t)$  follows a desired state trajectory  $\mathbf{x}_d(t)$ , starting from the same initial conditions. We can write the tracking error as a function of  $\mathbf{x}$ ; thus,

$$\tilde{\mathbf{x}} = \mathbf{x} - \mathbf{x}_d, \quad \dot{\tilde{\mathbf{x}}} = \dot{\mathbf{x}} - \dot{\mathbf{x}}_d = \begin{bmatrix} \dot{\tilde{x}} & \ddot{\tilde{x}} & \dots & \tilde{\mathbf{x}}^{(n-1)} \end{bmatrix}'$$

defining a manifold in the  $\mathbb{R}^n$  with the scalar relationship, where

$$\sigma(\mathbf{x}, t) = \left( \frac{d}{dt} + \lambda \right)^{n-1} \tilde{\mathbf{x}} \quad \text{with} \quad \lambda > 0 \quad (4)$$

then for a second-order system Eq. (4) becomes simply

$$\sigma = \dot{\tilde{x}} + \lambda \tilde{x} \quad (5)$$

The tracking problem becomes, therefore, that of assuring that the error state remains on  $\sigma(\mathbf{x}, t) = 0, \forall t > 0$ . The  $n$ -dimensional tracking problem becomes a one-dimensional stability problem with a control law that must satisfy the attractivity condition

$$\frac{0.5 d(\sigma^2)}{dt} \leq -\eta |\sigma| \quad (6)$$

outside the manifold, with  $\eta$  being a strictly positive constant. Equation (4) is also called an attractivity condition, reachable in a finite time even if the initial conditions at time zero are not satisfied. Once the manifold is reached, Eq. (4) ensures that the tracking error tends to zero asymptotically.

In addition to the general properties just described, the operator, given the error display, is capable of generating error rate information<sup>3</sup> and commutes his/her control action with a neuromuscular delay, known within rather precise boundaries. Because this investigation was preliminary in nature, a linear switching function for the operator  $\sigma = 0$  was first selected in the error space, and according to points 1 and 3, the resulting model structure was that of a constant amplitude relay, driven by error and error rate information. Performance comparison indicated discrepancy in the time histories because of the constant amplitude relay.

The selected model saturates at a threshold chosen as the value minimizing the mean squared error between the real control and the model itself. To reduce discrepancies in the amplitude and switching time, the model was modified with the introduction of an “adaptive relay” component as in Fig. 7. To identify the remaining parameters, the error and error rate were plotted in an error phase plane

$$\dot{e} + \gamma e = 0$$

as in Fig. 8, with switching (\*) and saturation (o) of control input taken from Fig. 6.

In the initial phase the operator determines the amount of control to be applied (during the training phase the amount of control increases until he/she realizes that the motion converges toward the switching surface, i.e.,  $\sigma \dot{\sigma} < 0$ ). Once the value is found, it is applied until the switching line is crossed and the control is reset to zero. The training phase of the operator was represented in the proposed model structure as a linear function of time (with slope  $k$ ) because the use of higher-order polynomials did not yield appreciable benefits. Because of the delay in human performance, switching occurs when the state has passed the line, as seen in Fig. 8.

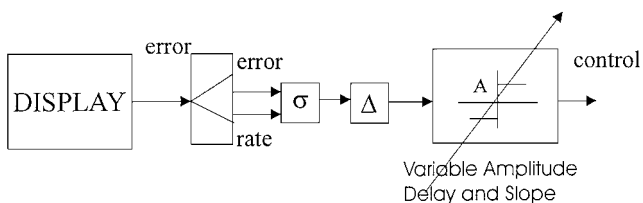


Fig. 7 Operator model.

Table 1 Parameters from operator A

| System parameters |          | Model parameters |          |        |
|-------------------|----------|------------------|----------|--------|
| $\xi$             | $\omega$ | $\kappa$         | $\gamma$ | $\tau$ |
| 0.5               | 0.2      | 15.04            | -64.90   | 0.09   |
| 0.2               | 0.4      | 32.54            | -68.40   | 0.08   |
| 0.2               | 0.8      | 16.3             | -70.78   | 0.08   |
| 0.2               | 1.0      | 9.7              | -72.62   | 0.08   |
| 0.2               | 2.0      | 13.41            | -73.43   | 0.07   |
| -0.2              | 0.2      | 11.55            | -56.66   | 0.07   |
| -0.2              | 0.4      | 13.1             | -57.80   | 0.09   |
| -0.2              | 0.8      | 11.44            | -58.50   | 0.05   |

Table 2 Parameters from operator B

| System parameters |          | Model parameters |          |        |
|-------------------|----------|------------------|----------|--------|
| $\xi$             | $\omega$ | $\kappa$         | $\gamma$ | $\tau$ |
| 0.5               | 0.2      | 3.25             | -28      | 0.27   |
| 0.2               | 0.4      | 3.05             | -31.6    | 0.29   |
| 0.2               | 0.8      | 1.6              | -40      | 0.28   |
| 0.2               | 1.0      | 0.87             | -56      | 0.32   |
| 0.2               | 2.0      | 3.0              | -54.7    | 0.20   |
| -0.2              | 0.2      | 3.38             | -24.6    | 0.34   |
| -0.2              | 0.4      | 3.5              | -16.8    | 0.25   |
| -0.2              | 0.8      | 1.65             | -40      | 0.18   |

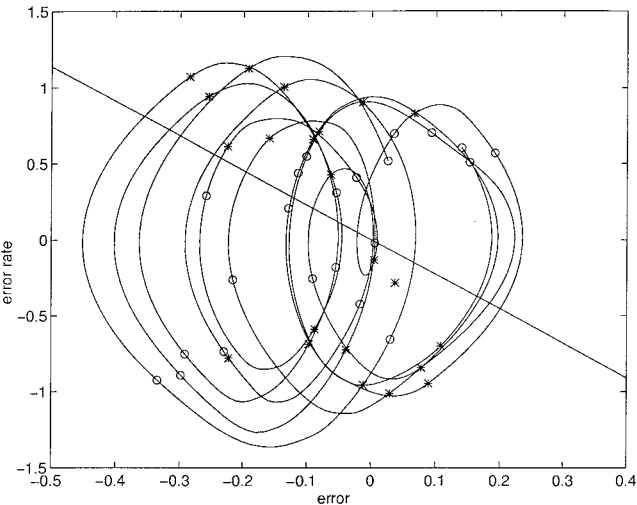


Fig. 8 Error behavior in the phase plane.

Identification of switching line  $\sigma = 0$  and delay  $\tau$  was performed by anticipating the switching times until a linear best fit of the switching distances was found. The training phase slope was obtained as the mean value of all slopes in the actual experiments. With the preceding procedure the modified error phase plane plot becomes that of Fig. 9.

The experimental values of the model parameters are given in Tables 1 and 2, indicating a more aggressive approach to the control by subject A compared to subject B.

IV. Validation

A series of four inputs consisting of a positive constant, a negative ramp, a negative constant, and a positive slope were given to extract limit-cycle information and to validate the model structure with experimental data. An example of the model time history vs real manual control action is shown in Fig. 10.

The model is capable of replicating the behavior of the manual controller in a satisfactory manner, especially because the control strategy becomes one of off type, with sign inversion in the control action and variable amplitude. Control inversion is associated with the crossing of a linear function in the error phase plane, and the delay is introduced by anticipating the commutation time until control inversion lies on the experimentally selected switching line.

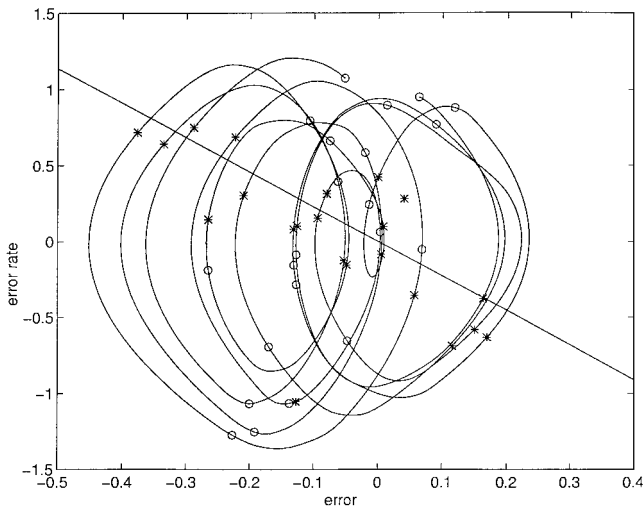


Fig. 9 Modified phase plane and switching line.

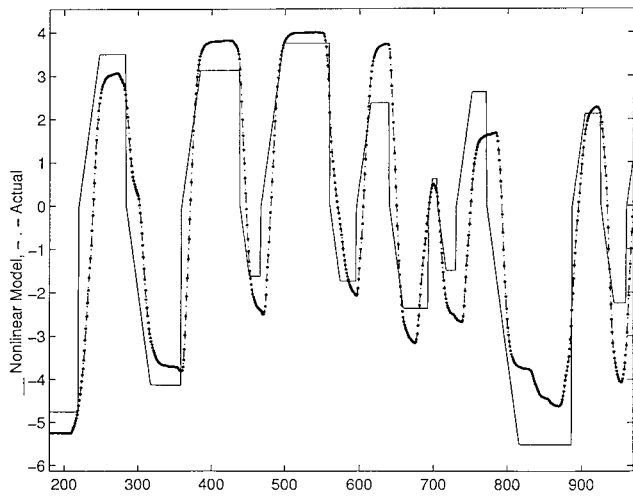


Fig. 10 Comparison between model and experimental control.

## V. Conclusions

A novel structure of a human operator in a control loop has been introduced, modeling manual control behavior in situations where such control requires a switching strategy. The model is based on an adaptive delayed relay structure with a linear switching line. Model parameters were obtained from a limited experimental database. Although preliminary in nature, the model shows performance consistent with the experimental data; the generality of the approach of course needs additional validation, and it may be limited to situations where operator control pulsing is clearly excited by appropriate input to the closed-loop system. The model identification parameters ( $k$ ,  $\gamma$ ,  $\tau$ ) appear candidate parameters to evaluate different operators' capabilities and training levels.

## Acknowledgments

This work was partially supported by the Italian Ministry of University, Scientific, and Technological Research under Grant MURST 40% "Control Engineering." The authors wish to thank Giovannoni and Folgarait for their valuable help in setting up the simulation facility and performing the experimental work.

## References

- <sup>1</sup>AGARD/NATO, "Advances in Flying Qualities," AGARD-LS-157, Lecture Series, May–June 1988.
- <sup>2</sup>McRuer, D. T., and Krendel, E. S., "Human Dynamics in Man-Machine Systems," *Automatica*, Vol. 16, 1980, pp. 237–253.
- <sup>3</sup>Hess, R. A., "Structural Model of the Adaptive Human Pilot," *Journal of Guidance, Control, and Dynamics*, Vol. 3, No. 5, 1980, pp. 416–423.
- <sup>4</sup>Innocenti, M., "The Optimal Control Pilot Model and Application," AGARD LS-157, Lecture Series, Lecture No. 8, May–June 1988.
- <sup>5</sup>Davidson, J. B., and Schmidt, D. K., "Modified Optimal Control Pilot Model for Computer-Aided Design and Analysis," NASA-TM-4384, 1992.
- <sup>6</sup>MacAdam, C., "Application of an Optimal Preview Control for Simulation of Closed Loop Automobile Driving," *IEEE Transactions on Systems, Man, and Cybernetics*, Vol. 11, June 1981, pp. 393–400.
- <sup>7</sup>Sheridan, T. B., and Ferrell, W. R., *Man-Machine Systems: Information, Control, and Decision Models of Human Performance*, Massachusetts Inst. of Technology Press, Cambridge, MA, 1974.
- <sup>8</sup>Innocenti, M., Balluchi, A., and Balestrino, A., "New Results on Human Operator Modelling During Nonlinear Behavior in the Control Loop," American Control Conference ACC97, July 1997.
- <sup>9</sup>Utkin, V., *Sliding Modes and Their Application in Variable Structure Systems*, MIR, Moscow, 1978.
- <sup>10</sup>Slotine, J.-J. E., and Li, W., *Applied Nonlinear Control*, Prentice-Hall, Upper Saddle River, NJ, 1991.

## Experiments on Space Robot Arm Path Planning Using the Sensors Database, Part II

Toshiaki Iwata\*

Electrotechnical Laboratory, Ibaraki 305-8568, Japan

Seiya Ueno†

Yokohama National University, Yokohama 240-8501,

Japan

and

Hiroshi Murakami‡

Electrotechnical Laboratory, Ibaraki 305-8568, Japan

## Introduction

THE orientation of a free-flying space robot is disturbed by the arm movement. However, the space robot can simultaneously control the orientation of its main body and arm position using only arm motion due to its nonholonomic constraints.<sup>1–4</sup> We have presented path-planning methods such as breadth-first search and A\* search, using a sensor-motion database, which are not model-based methods but sensor-based ones.<sup>1</sup> However, the breadth-first search required a long time to determine the path, and A\* search did not always indicate the shortest solution or did not find the path at all. These methods yielded the path only after a successful search, so that the search could not be terminated halfway. In actual situations, because the tasks of the space robot will be composed of a series of planned motions, the paths should be short and planned in a short time even though they may not be the shortest possible. The genetic algorithm (GA), which uses the same database as that of the previous search methods, yields a temporary path in a short time. Furthermore, because the database is specific to discrete joint angles, it is not possible to accommodate arbitrary continuous values. This presents a serious problem. Therefore, we approximate the relationships between sensor states and robot motions in the database using a formula and use optimal control techniques with the formula to deal with continuous joint angle values.

## Path-Planning Methods

The space robot situation considered and the database used in the experiments are the same as those shown in Figs. 1 and 2 of Ref. 1

Received 18 December 1998; revision received 16 December 1999; accepted for publication 7 February 2000. Copyright © 2000 by the authors. Published by the American Institute of Aeronautics and Astronautics, Inc., with permission.

\*Senior Researcher, Frontier Technology Division, 1-1-4 Umezono, Tsukuba. Senior Member AIAA.

†Associate Professor, Division of Artificial Environment and Systems, 79-5 Tokiwadai, Hodogaya-ku. Member AIAA.

‡Senior Researcher, Frontier Technology Division, 1-1-4 Umezono, Tsukuba.